HHS Public Access

Author manuscript

Cell Rep. Author manuscript; available in PMC 2020 February 26.

Published in final edited form as:

Cell Rep. 2020 February 11; 30(6): 1923–1934.e4. doi:10.1016/j.celrep.2020.01.047.

CCL2 and CXCL12 Derived from Mesenchymal Stromal Cells Cooperatively Polarize IL-10+ Tissue Macrophages to Mitigate Gut Injury

Jayeeta Giri[1], **Rahul Das**[1], **Emily Nylen**[2], **Raghavan Chinnadurai**[3], **Jacques Galipeau**[1,4,*]

[1]Department of Medicine, University of Wisconsin Carbone Comprehensive Cancer Center, University of Wisconsin-Madison, Madison, WI 53705, USA

[2]Medical College of Wisconsin, 8701 W Watertown Plank Road, Wauwatosa, WI 53226, USA

[3]Department of Biomedical Sciences, Mercer University School of Medicine, Savanah, GA 31324, USA

[4]Lead Contact

SUMMARY

Mesenchymal stromal cell (MSC)-based therapy for inflammatory diseases involves paracrine and efferocytotic activation of immunosuppressive interleukin-10$^+$ (IL-10$^+$) macrophages. The paracrine pathway for MSC-mediated IL-10$^+$ macrophage functionality and response to tissue injury is not fully understood. In our present study, clodronate pre-treatment of colitic mice confirms the essential role of endogenous macrophages in bone-marrow-derived MSC (BM-MSC)-mediated clinical rescue of dextran sulfate sodium (DSS)-induced colitis. We identify that BM-MSC-secreted chemokine ligand 2 (CCL2) and C-X-C motif chemokine 12 (CXCL12) cooperate as a heterodimer to upregulate IL-10 expression in CCR2$^+$ macrophages *in vitro* and that CCL2 expression by MSC is required for IL-10$^+$ polarization of intestinal and peritoneal resident macrophages *in vivo.* We observe that tissue macrophage IL-10 polarization *in vivo* is widespread involving extra-intestinal tissues and secondarily leads to bystander IL-10 expression in intestine-resident B and T cells. In conclusion, the BM-MSC-derived chemokine interactome dictates an IL-10$^+$-macrophage-amplified anti-inflammatory response in toxic colitis.

In Brief

*Correspondence: jgalipeau@wisc.edu.

AUTHOR CONTRIBUTIONS

J. Giri designed the research plan, performed experiments, analyzed results, and wrote the manuscript; R.D. assisted in tissue culture and immunoprecipitation study; E.N. provided technical support in the animal study; R.C. generated pilot data and administrative support; and J. Galipeau supervised the project, designed the research plan, analyzed results, and wrote the manuscript.

DECLARATION OF INTERESTS

The authors declare no competing financial interests.

SUPPLEMENTAL INFORMATION

Supplemental Information can be found online at https://doi.org/10.1016/j.celrep.2020.01.047.

Giri et al. show that the chemokines CCL2 and CXCL12, secreted from bone-marrow-derived mesenchymal stromal cells, upregulate IL-10 expression in $CCR2^{+}$ macrophages. These polarized macrophages reduce tissue inflammation in colitis.

Graphical Abstract

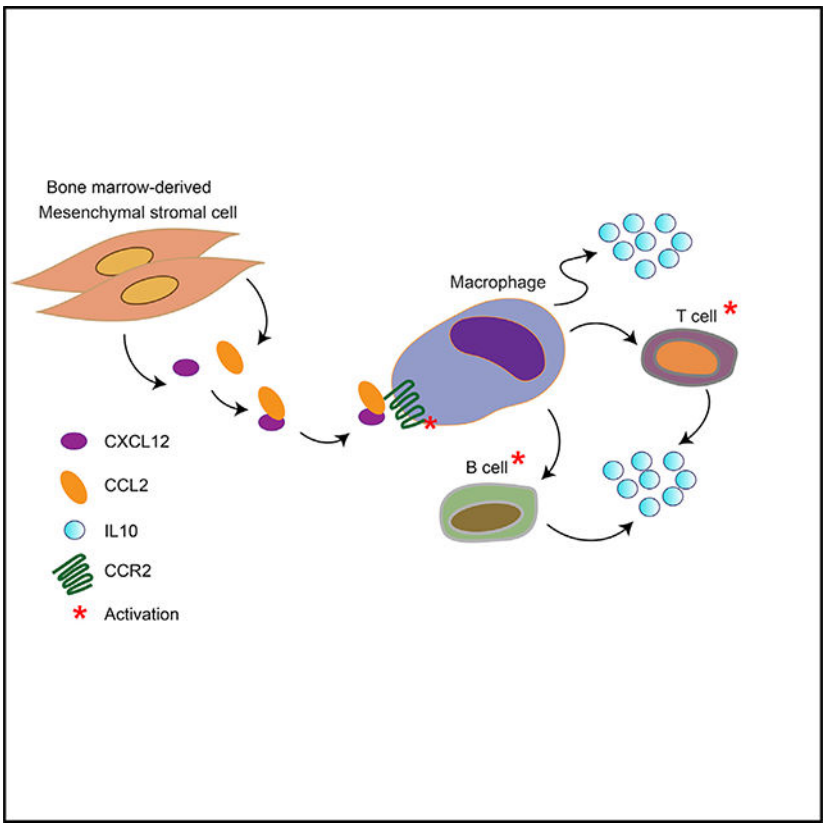

INTRODUCTION

Culture-adapted bone-marrow-derived mesenchymal stromal cells (BM-MSCs) are a polyclonal population of adult stromal cells that display regenerative and immunomodulatory properties, supporting their clinical study as a cellular pharmaceutical (Galipeau and Sensébé, 2018). Based on their immune suppressive competency, the use of BM-MSCs as a transfusion product to treat immune disorders, including inflammatory bowel disease (IBD), has been the subject of intense clinical investigation (Ciccocioppo et al., 2019; Grégoire et al., 2017).

Adoptive transfer of culture-adapted autologous and allogeneic BM-MSC, as well as MSCs from an adipose source, have demonstrated unequivocal effectiveness in improving clinical outcomes in pre-clinical murine models of intestinal injury (Chinnadurai et al., 2015). Although imperfect, these pre-clinical model systems provide supporting data for the translational use of MSCs for IBD as well as mechanistic insights, such as a pivotal role for endogenous tissue macrophages as part of the therapeutic response to MSCs (Song et al.,

2017b). Human clinical trials examining intravenous delivery of MSCs for IBD have had mixed therapeutic outcomes with the notable exception of adipose-derived MSCs for locoreginal treatment of Crohn-associated perianal fistular disease (Panés et al., 2016, 2018b). The ADMIRE CD study validated the pivotal concept of MSC fitness as an essential component to their clinical effectiveness, providing the impetus to better understand MSC functionality in improving their utility in treatment of IBD and related inflammatory disorders.

In the healthy intestine, the immune-suppressive M2 macrophage phenotype dominates over the M1 phenotype, whereas resident macrophages show an inflammatory M1 phenotype in the inflamed intestinal mucosa (Hidalgo-Garcia et al., 2018). M2 macrophages maintain this homeostasis by secreting the major anti-inflammatory cytokine interleukin-10 (IL-10) (Hidalgo-Garcia et al., 2018). Deletion of the IL-10 receptor in macrophages causes severe colitis in mice at a similar extent as colitis developed in IL-$10^{-/-}$ or IL-$10Ra^{-/-}$ mice (Li et al., 2014). In light of these observations, a plausible MSC-mediated therapeutic effect in colitis may be to convert the balance of the recipient's intestinal macrophage populations into the IL-10-producing and -responsive M2 phenotype (Cho et al., 2014).

BM-MSC's *in vitro* immunomodulatory effects are mostly driven by their paracrine effects through the secretion of a range of cytokines, chemokines, and other soluble and contact factors (Galipeau and Sensébé, 2018). Among these, we have previously demonstrated that BM-MSC-derived chemokine ligand 2 (CCL2) is necessary to reverse neuroinflammation in a murine model of experimental autoimmune encephalitis (EAE) and is further required to dampen encephalitogenic $CCR2^+$ CD4 Th17 cells (Rafei et al., 2009). The same MSC/CCL2 axis was shown to mediate the suppression of experimental alloimmunization by endogenous $CCR2^+$-santibody-producing cells *in vivo* (Rafei et al., 2008). Previous seminal pre-clinical studies have shown that murine BM-MSC can promote lung-tissue-resident macrophage class switching toward an IL-10^+ M2 phenotype (Németh et al., 2009), speaking to the pivotal importance of host macrophages as part of the MSC-driven immune-suppression response. Intriguingly, CCL2 upregulation by marrow-resident CXCL12 abundant reticular (CAR) cells in mice also plays a key role in monocyte mobilization *in vivo* (Shi et al., 2011), suggesting a fundamental biological role of BM-MSC CCL2 chemokine expression in modulating monocyte functionality. However, the detailed molecular mechanism of the cross-talk between chemokines provided by exogenous MSC adoptive transfer and host tissue macrophages remains undefined.

Here, we demonstrate that murine BM-MSCs deploy a functional chemokine interactome where CCL2 and C-X-C motif chemokine 12 (CXCL12) cooperativity dictate IL-10^+ macrophage polarization in a CCR2-dependent manner. The effect of BM-MSCs on host tissue macrophages extends beyond inflamed bowel and further deploys a cascade of IL-10 upregulation in tissue resident B cells and T cells. These observations provide mechanistic information on the pharmacology of BM-MSC adoptive transfer that likely extends to other acute tissue injury and inflammatory syndromes.

RESULTS

Clodronate-Sensitive Macrophages Are Essential for the Therapeutic Effect of Intraperitoneal-Delivered BM-MSCs in DSS-Induced Colitis

Although MSCs are known to promote macrophage M1 to M2 class switching, it is not known whether these cells are required for the effects of BM-MSCs on the clinical outcome of colitis. To address this question, we used a dextran sulfate sodium (DSS)-induced colitis mouse model to first establish the effect of intraperitoneal adoptive transfer of culture-adapted BM-MSCs in curbing disease severity. In line with previous studies (Sala et al., 2015), intraperitoneal injection of 10×10^6 syngeneic BM-MSCs into C57BL/6 mice after 2 and 4 days of DSS treatment significantly improved clinical parameters, such as body weight (Figure 1B), disease activity index (Figure 1C), and histological scores (Figures 1D and 1E), compared with mice treated with phosphate-buffered saline (PBS). Importantly, interferon γ (IFNγ) licensing increased the efficacy of MSCs, as reflected by reduced disease severity in an IFNγ-pretreated MSC-transfused group compared to a resting MSC group, which is corroborated by previous reports showing IFNγ priming improves the potency of MSCs (Duijvestein et al., 2011). To evaluate whether host macrophages are required for exerting the therapeutic effect of BM-MSCs, B6 mice were administered an intravenous injection of clodronate-loaded liposome (Clo-lip) 24 h before DSS treatment and compared to liposome vehicle control (lip) in their subsequent response to BM-MSCs. Clodronate-treated mice developed severe colitis and were unresponsive to BM-MSCs relative to control mice, as demonstrated by an indistinguishable effect on body weight loss (Figure 1G), disease activity index (Figure 1H), and histological scores (Figures 1I and 1J). These data support the hypothesis that endogenous monocytes/macrophages are necessary mediators of BM-MSC-dependent reduction of colitis severity.

The BM-MSC Secretome Induces Peritoneal Macrophage M2 Polarization That Is Functionally Dependent on IL-10 Expression for Bystander T Cell Suppression

Considering the pivotal role of endogenous macrophages in improving DSS colitis following intraperitoneal adoptive transfer of BM-MSCs, we analyzed the direct paracrine cross-talk of BM-MSC with peritoneum-resident macrophages. To address this question, we examined the effect of BM-MSC condition media (MSC-CM) on *in-vitro-culture-adapted* peritoneal-cavity-derived macrophages (PMϕ). Following 24 h of exposure to MSC-CM, flow cytometric analysis of treated PMΦ revealed that $CD45.2^+/CD11b^+$ dual-positive PMΦ significantly increased the expression of CD206 and CD163 (from 2.0% ± 0.2% to 20.8% ± 0.2% and from 1.9% ± 0.3% to 20.9% ± 0.7%, respectively) and significantly reduced CD86 and iNOS expression as well (99.6% and 63.5%, respectively) when compared to lipopolysaccharide (LPS)/IFNγ-treated PMΦ (Figures 2A and 2B). LPS/IFNγ-treated PMϕ adopt a M1-polarized phenotype (Müller et al., 2017) and served as a comparator control. Contemporaneous analysis of IL-10 production by PMϕ revealed a ~8-fold increase in expression upon MSC-CM treatment compared to LPS/IFNγ treatment (Figure 2C), which was further ~3-fold enhanced by BM-MSC IFNγ prelicensing (Figure 2D). Removal of MSC-CM from PMϕ led to depolarization to a M0 phenotype within 24 h (Figure 2E).

We further studied the effect of MSC-CM-polarized PMϕ as suppressors of T cell proliferation by co-culturing with activated T cells. We observed 93.6% ± 1.7% and 17.62% ± 2.0% Ki67-positive T cells in control and T cells cocultured with MSC-CM-treated PMϕ, respectively (Figure 2F). To assess the role of PMϕ-derived IL-10, PMϕ derived from IL-10$^{-/-}$ mice were conditioned with MSC-CM and co-cultured with activated T cells. IL-10$^{-/-}$ PMϕ paradoxically stimulated T cell proliferation by ~2-fold compared to naive PMϕ, which suggests that T cell suppressor function is partially regulated by PMϕ-derived IL-10.

BM-MSC-Derived CCL2 Induces Macrophage M2 Polarization

Considering the previously defined role of BM-MSC-derived CCL2 in affecting outcomes in pre-clinical murine models of auto and alloimmune disorders (Rafei et al., 2008, 2009) and further considering its potential in macrophage recruitment (Shi et al., 2011) and polarization (Roca et al., 2009), we interrogated its role in the context of MSC/PMϕ interaction. Both resting and cytokine-primed MSCs secrete CCL2, which levels are respectively ~7- and ~16-fold higher than basal culture media, as measured by ELISA (Figure 3A). CCL2 produced by BM-MSC is necessary for the induction of IL-10 expression by macrophages *in vitro* because the use of neutralizing anti-CCL2 antibody abolishes PMϕ polarization (Figure 3B). To further validate the role of CCL2 on responsive CCR2^{+} PMϕ, we treated PMϕ with the CCR2 inhibitor (RS2085) contemporaneously to MSC-CM conditioning, which resulted in significantly reduced IL-10 production (Figure 3C), with inhibition observed within 6 h of RS2085 pre-treatment and maximal at 24 h (Figure 3C). To investigate the role of CCL2 in BM-MSC-mediated recovery of DSS-induced colitis, we isolated BM-MSCs from CCL2$^{-/-}$ mice and infused them into DSS-treated syngeneic mice. Compared to controls, these mice failed to improve colitis, as depicted by body weight loss (Figure 3E), disease activity index (Figure 3F), and histological scores (Figure 3G).

MSC-Secreted Chemokines CCL2 and CXCL12 Synergistically Induce Macrophage M2 Polarization

To gain further insight into the mechanism of CCL2-mediated PMϕ M2 polarization, we interrogated the effect of recombinant CCL2 (rCCL2) as an *in vitro* inducer of IL-10 production by PMϕ. Surprisingly, rCCL2-treated PMϕ did not upregulate IL-10 expression relative to controls (Figure 4A). Considering previous reports that BM-MSC-derived metalloproteinase (MMP) process CCL2 to generate an N-terminal-cleaved form of CCL2 with anti-inflammatory functionality (Ho et al., 2009, 2014; Rafei et al., 2008), we tested whether coincubation of rCCL2 and MMP1 would induce IL-10 expression by PMϕ without avail (Figure 4B). An alternate hypothesis was that MSC-CM media contain a factor that acts in complementation with CCL2 to induce IL-10 expression by PMϕ. To verify this, we treated PMϕ with MSC-CM derived from CCL2$^{-/-}$ BM-MSCs in combination with rCCL2. Interestingly, the addition of rCCL2 to CCL2$^{-/-}$ MSC-CMs induced substantial IL-10 production in PMϕ in a dose-dependent manner when compared rCCL2 monotreatment (Figure 4C). This result indicates that CCL2 in BM-MSCs is necessary but not sufficient for IL-10 production by PMϕ. It has been reported that CCL2 and other chemokines can form heteromeric quaternary complexes and synergize to amplify the effect of CCL2 on target

cells (Gouwy et al., 2008; Proudfoot and Uguccioni, 2016). Considering that culture-adapted BM-MSCs constitutively produce an array of chemokines, including CXCL12, CCL7, CCL9, and CXCL4, we speculated that CCL2 may interact with one of those chemokines to enhance IL-10 production by PMϕ. To investigate this hypothesis, we concentrated MSC-CMs, treated them with an ethylene glycol bis(succinimidyl succinate) (EGS) cross-linker followed by immunoprecipitation (IP) with an anti-CCL2 antibody (Figure 4D), and performed immunoblot analysis. Surprisingly, western blot analysis of CCL2-IP MSC-CMs showed a clear expression of CCL2 (Figure S1A), whereas EGS-cross-linked and CCL2-IP MSC-CMs revealed bands at higher molecular weight at two different positions (Figure 4D), which suggested CCL2 homo or heterodimeric forms. To identify the binding partner(s) of CCL2 in MSC-CMs, we analyzed MSC-CMs IP with either anti-CCL2 or anti-CXCL12 antibodies with chemokine arrays (Figures 4E–4H). First, we added external rCCL2 in the concentrated MSC-CMs to increase the abundance of CCL2 to its binding partner. The addition of rCCL2 to MSC-CM led to robust CXCL12 pull-down as detected by array (Figure S1B). To validate the physiological relevance of this result, we repeated this IP study in the absence of excess exogenous rCCL2 and observed qualitative pull down of CXCL12 (Figure 4E), which was further amplified when using CM from IFNγ-licensed BM-MSCs, which leads to increased CXCL12 production by the same cells (Figures S2A and S2B, respectively). Interestingly, CXCL12-IP MSC-CMs showed moderate expression of CCL2, indicating the molar interaction ratio of CXCL12/CCL2 is >1 (Figure 4F). To validate the specificity of our findings, we repeated this array pull-down experiment with anti-CCL2-IP MSC-CM derived from $CCL2^{-/-}$ bone-marrow-derived MSC (BM-MSC). As expected, no protein pull down was observed in this array study (Figure 4G). Chemokine array analysis of CXCL12-immunoprecipiated MSC-CMs derived from $CCL2^{-/-}$ BMSCs led to IP of CXCL12, but no other protein was co-IP (Figure 4H). To quantify the amount of CCL2 interacting with CXCL12, we performed an ELISA assay on both CCL2- and CXCL12-IP MSC-CMs, where we found that CXCL12 at a concentration of 2,152.7 ± 15.3 pg/ml (Figure 4J) interacts with CCL2 at a concentration of 227.4 ± 3.3 pg/ml (Figure 4I). To validate the functional role of CXCL12 as part of the CCL2/CXCL12 cooperativity, we added a neutralizing anti-CXCL12 antibody to MSC-CM and observed that it significantly inhibited IL-10 expression by responsive PMϕ (Figure 4K). To define the role of CXCR4 (the receptor for CXCL12) in the polarization of M2 macrophages by MSC CM, we treated macrophages *in vitro* with a CXCR4 inhibitor, and after 24 h, we collected the supernatant and performed an IL-10 ELISA. As shown in Figure S3, blockade of CXCR4 signaling did not prevent the induction of IL-10 by MSC-CM. These data support the hypothesis that the CCL2/CXCL12 heterodimer deploys its functionality solely through CCR2. To strengthen the evidence of cooperativity of CCL2 and CXCL12 on M2 polarization, we tested the dose/response of the rCCL2 and rCXCL12 combination on IL-10 induction by PMϕ. Interestingly, rCCL2 at a concentration of 1 ng/ml in combination with rCXCL12 at a concentration of 300 ng/ml gave the maximum induction of IL-10 production by PMϕ (Figure 4L). Therefore, our findings altogether suggest that MSC-CM-derived CCL2 and CXCL12 can form heterodimers and further synergize to induce PMϕ $IL\text{-}10^{+}$ M2 polarization (Figure 4M).

Host IL-10 Competency Is Indispensable for MSC-Mediated Recovery of DSS Colitis

Because IL-10 is a major anti-inflammatory cytokine with a role in maintaining gastrointestinal homeostasis, we tested whether host-derived IL-10 is important for the actions of adoptively transferred BM-MSCs *in vivo.* To address this question, we induced DSS colitis in IL-$10^{-/-}$ mice and administered 10×10^6 syngeneic BM-MSCs IP to the mice at 2 and 4 days following the start of DSS treatment. All of the BM-MSC-treated IL-$10^{-/-}$ colitic mice displayed substantially worse colitic morbidity and mortality relative to IL-10-sufficient mice. In contrast, BM-MSC-treated IL-10-competent mice displayed significantly reduced body weight loss (Figure 5B). BM-MSC-treated colitic IL-$10^{-/-}$ mice developed a substantially worse disease activity index score (Figure 5C) and severe inflammatory infiltrates into colon, a disruption of crypt architecture as measured by histological score (Figure 5, D–E), when compared to IL-10-competent colitic mice. As an aggregate, our data confirm the pivotal role of host IL-10 in the BM-MSC-mediated effect on colitis outcomes.

BM-MSC-Polarized Host Macrophages Secondarily Mobilize IL-10^+ Gut- and Tissue-Resident T and B Cells

Based on the above results, we hypothesized that BM-MSCs mitigate DSS colitis by inducing host immune cells capable of producing IL-10. To test our hypothesis, we generated colitis in a GFP/IL-10 (Vert-X) reporter mouse model (Madan et al., 2009) to serve as a means to identify IL-10-secreting immune cells *in vivo.* In these mice, we subsequently injected 10×10^6 BM-MSC IP on days 2 and 3 following the start of DSS treatment. On day 4, we isolated intestinal and peritoneal cavity cells and assessed GFP/IL-10 expression of gut and peritoneal cavity resident CD11b, F4/80 double-positive macrophages, and CD3-positive T and B220-positive B cells by flow cytometric analysis. We observed that both intestinal- and peritoneal-cavity-derived macrophages (19.6% ± 3.0% and 11.4% ± 0.7% respectively), T cells (15.9% ± 4.7% and 10.3% ± 1.6%, respectively), and B cells (18.8% ± 3.2% and 14.9% ± 2.8% respectively) express a substantially higher percentage of GFP/IL-10 in BM-MSC-treated mice relative to controls (Figures 6A–6D). However, GFP/IL-10 expression was lost 72 h post-BM-MSC adoptive transfer (Figure S4). The *in vivo* IL-10 polarization of gut-resident host macrophages and T cells was dependent on CCL2 produced by transferred MSCs because CCL2$^{-/-}$ MSCs failed to upregulate such (Figure S5). Because host macrophages are essential for the therapeutic effect of BM-MSCs (Figures 1F–1J), we asked whether this IL-10 induction by bystander gut and peritoneal B and T cells is macrophage dependent or not. To test this hypothesis, we depleted macrophages by administering Clo-lip into Vert-X reporter mice before DSS treatment and subsequent adoptive transfer of BM-MSCs. Interestingly, we found that depletion of clodronate-sensitive host macrophages significantly reduced the percentage of IL-10 producing T (1.7% ± 1.1% and 2.7% ± 1.7% in intestine and peritoneal cavity, respectively) and B cells (0.7% ± 0.3% and 2.6% ± 1.0% in intestine and peritoneal cavity, respectively) in BM-MSC-treated colitic mice compared to controls (Figures 6E–6H). These data altogether suggest that MSC-polarized host macrophages are a key intermediate in IL-10 expression by bystander tissue T and B cells.

DISCUSSION

The ADMIRE CD clinical trial demonstrated that administration of 120 million allogeneic adipose stromal cells within Crohn-associated enterocutaneous fistulas and surrounding soft tissues leads to healing and closure with significant clinical benefit (Panés et al., 2018a). These data informed the first marketing approval of MSCs as a living cell pharmaceutical by the European Medicines Agency (Sheridan, 2018; Hoogduijn and Lombardo, 2019). The inclusion criteria in the study required that subjects and controls have quiescent gut luminal disease with a Crohn's Disease Activity Index (CDAI) of <220. Indeed, the baseline mean CDAI in both groups was 90, and the incidence or relapsed luminal disease during the course of study was nearly absent. Therefore, the study design was not powered to assess the impact of MSC administration on recurrent systemic and gut luminal Crohn disease over the 12-month observation (J. Panes, personal communication). However, the substantial clinical benefit of MSCs in resolving Crohn-associated inflammatory fistular pathology in humans foreshadows the possibility that active systemic luminal disease may be responsive or preventable as well. In support of this hypothesis, there is a substantial amount of published data that extravascular delivery of MSCs improves outcomes in pre-clinical rodent models of toxic colitis (Chinnadurai et al., 2015). The knowledge gap lies in defining the cell biology properties of adoptively transferred MSCs that define their potency as anti-inflammatory cell drug pharmaceuticals *in vivo.*

We show that *in vivo* depletion of clodronate-sensitive host tissue macrophages obviates the therapeutic effects of BM-MSCs in DSS colitis (Figures 1F–1J). This observation speaks to the pivotal MSC and host macrophage cross-talk and that macrophage responsiveness is systemic despite compartmentalized (e.g., intraperitoneal) delivery of MSCs. Although efferocytosis of MSCs by macrophages has been proposed to provide cell-function-autonomous immune modulation, the secretome of biologically fit MSCs would best explain the macrophage responsiveness in tissue compartments where efferocytosis is not plausible by virtue of route of delivery or where MSC tissue homing is nearly absent. In support of this hypothesis, we also found that intraperitoneal administration of heat-inactivated (killed) BM-MSCs failed to improve colitis outcomes in DSS-treated mice (data not shown). Considering the established role of MSC-produced chemokines, CCL2 in particular, in modulating the biology of responsive lymphomyeloid cells (Lee et al., 2017; Rafei et al., 2008; Takeda et al., 2018), we focused on this cell biological property to define its role in paracrine MSC/macrophage interplay. We show that the secretome of BM-MSCs is sufficient to polarize primary peritoneal macrophages to the IL-10^{+} M2 phenotype that supports the efferocytosis-autonomous paracrine functionality of MSCs (Figures 2A–2D). The loss of *in vitro* M2 polarizing competency of $CCL2^{-/-}$ BM-MSC (Figure 4C) speaks to the necessity of MSC-borne CCL2, which is further supported by the observation that the secretome of $CCL2^{+/+}$ MSC treated with neutralizing anti-CCL2 antibody loses M2 polarizing competency as well (Figure 4K). Macrophages are known to express a plurality of chemokine receptors, including CCR2 (Mantovani et al., 2004; Varol et al., 2015). Chemokines, including CCL2, are promiscuous in their use of chemokine receptors, allowing for a complex interactome (Hughes and Nibbs, 2018; Miller and Mayo, 2017). With the use of the specific CCR2 small-molecule-inhibitor RS 102895, we show that CCR2

function by responder macrophages is necessary to mediate CCL2-driven M2 polarization (Figure 3C). The relevance of these *in vitro* findings is further supported by the loss of function of $CCL2^{-/-}$ MSCs in affecting colitis outcome *in vivo* (Figures 3D–3G).

Surprisingly, rCCL2 on its own failed to polarize peritoneal macrophages *in vitro* (Figure 4A) even when processed by MMPs, which are known to activate the suppressor function of N-terminal-cleaved CCL2 (Ho et al., 2009; Rafei et al., 2008) (Figure 4B). However, rCCL2 functionality was rescued by complementation with the secretome derived from $CCL2^{-/-}$ MSCs (Figure 4C), suggesting that CCL2 potency was dependent upon complementation by a non-CCL2 soluble factor found in MSC-tconditioned media. It is known that chemokines such as CCL2 will spontaneously form in solution quaternary higher order structures including homodimers as well as heterodimers with other chemokines (Gouwy et al., 2008; Miller and Mayo, 2017; Nesmelova et al., 2008). To identify potential CCL2 heteromeric partners in the MSC secretome, we used a protein cross-link and CCL2 pull-down approach followed by a chemokine array screen of immunoprecipitate and identified CXCL12 as a consistent CCL2-associated chemokine (Figure 4E). This observation was supported by synergy of the rCCL2 and CXCL12 combination in inducing IL-10 expression by macrophages *in vitro* (Figure 4L). CXCL12 is unique among all chemokines in that it is the only member of this protein family whose absence is embryonic lethal (Karpova and Bonig, 2015), which speaks to its biological relevance in development and postnatal functionality. We further validated the importance of CXCL12 cooperativity with CCL2 by use of an anti-CXCL12 neutralizing antibody that abolished the polarizing properties of the MSC secretome (Figure 4K). Interestingly, blockade of CXCR4 still allowed macrophage polarization by the MSC secretome (Figure S3), speaking to the unique role of CCR2 in polarizing macrophages in response to CCL2/CXCL12 heterodimers. As an aggregate, these *in vitro* data show that MSC-borne CCL2 and CXCL12 cooperate, likely as a heterodimer, by CCR2 expressed by tissue macrophages, leading to IL-10 expression as part of an M2-polarized phenotype and that the phenomenon is reversible within 24 h of withdrawal of the MSC secretome.

We show that mouse IL-10 competency is essential considering the unresponsiveness of colitic $IL\text{-}10^{-/-}$ mice to adoptively transferred MSCs (Figures 5A–5E). To better define the downstream effects of MSC on IL-10 induction *in vivo,* we used the Vert-X mouse that will selectively co-express GFP in cells that contemporaneously upregulate IL-10 production (Madan et al., 2009). The analysis of peritoneal and gut-resident lymphomyeloid cells in colitic Vert-X mice treated with MSCs demonstrated that resident macrophages and B- and T cells expressed IL-10 (Figures 6A–6D). Clodronate pre-treatment of these mice abolished the induction of IL-10 expression in peritoneal and gut-resident bystander tissue-resident lymphoid cells. This latter observation places macrophages at the nexus of MSC-associated induction of IL-10 by tissue-resident lymphoid cells *in vivo.* Previous published work suggests that macrophage-borne IL-10 (Chiossone et al., 2016), indoleamine 2, 3-dioxygenase (IDO) (Vasandan et al., 2016) and CCL18 (Melief et al., 2013) may be candidate pathways through which MSC-polarized macrophages induce IL-10 expression in bystander tissue-bound lymphoid cells.

Published reports examining native bone-marrow-resident MSCs at the single-cell level confirm that both platelet-derived growth factor receptor (PDGFR)-expressing mice (Tikhonova et al., 2019) and human BM-MSCs (Ghazanfari et al., 2016) constitutively express CXCL12. Indeed, CXCL12 derived from Nestin-expressing mouse MSCs plays an essential role for hematopoietic stem cell (HSC) maintenance and retention in the bone marrow (Asada et al., 2017). Interestingly, marrow-endogenous mouse BM-MSCs do not express CCL2 unless stimulated with a TLR agonist (Shi et al., 2011), in contrast to robust constitutive expression of CCL2 as well as CXCL12 in culture-adapted and expanded BM-MSCs (Chinnadurai et al., 2018). Indeed, culture-adapted BM-MSCs share features with the endogenous $PDGFR^{+}$ progenitors from which colony-forming units (CFUs) arise (Farahani and Xaymardan, 2015; Matsuzaki et al., 2014) but deploy functionalities likely arising from mitogenic stimulation by PDGF and other growth factors typically found in serum-based culture expansion of MSCs for pharmaceutical use. It has also been reported that MSC-expressed tumor necrosis factor-inducible gene 6 (TSG-6) is necessary for macrophage polarization (Song et al., 2017b). Because it is known that TSG-6 can associate with chemokines by their glycosaminoglycan (GAG)-binding domain and alter chemokine functionality (Dyer et al., 2016), it is possible that higher order quaternary structures involving chemokines and associated proteins such as TSG-6 produced by MSCs are part of the chemokine interactome (Miller and Mayo, 2017) generated by culture-adapted MSCs.

Our *in vivo* delivery of metabolically fit MSCs in mice was intraperitoneal. Similar results were obtained when MSCs are administered subcutaneously (data not shown), and the effect of MSCs was absent in mice treated intravenously (data not shown). These data are consistent with the observation that route of delivery has a major impact on MSC potency in pre-clinical disease models (Caplan et al., 2019). Furthermore, the extravascular depot of MSCs IP or subdermally as shown here or possibly intramuscular may serve as potent substitutes to the intravenous route when seeking a systemic immune modulatory response. It has been shown that the *in vivo* persistence of fit MSCs is short (<3 days) following intravenous (i.v.) delivery and intermediate (7–21 days) following either intraperitoneal or subdermal route and the use of thawed MSCs dramatically shortens *in vivo* persistence (Braid et al., 2018). Indeed, the triggering of the instant-blood-mediated inflammatory reaction (IBMIR) following intravenous administration of MSCs may well lead to substantially mitigated persistence *in vivo*, especially if MSCs are administered immediately post-thaw (Moll et al., 2019). Considering that the ADMIRE CD study (Panés et al., 2018a) utilized metabolically fit culture-rescued MSCs in lieu of thawed cells and that MSCs were delivered subdermally, it may provide some insight on the importance of route of delivery and cellular metabolic fitness on MSC persistence *in vivo* (Galipeau and Sensébé, 2018). Furthermore, considering that MSCs deploy a systemic response despite local delivery speaks to the biologically plausible theorem supported by our data that the production of secreted leukines, such as CCL2/CXCl12, can act at a distance on tissue macrophages poised for responsiveness and such may be further enabled by cargo-bearing MSC-borne exosomes (Shi et al., 2018).

The adoptive transfer of killed or apoptotic MSCs will lead to a cell-function-autonomous immune-suppressive effect (Galleu et al., 2017), likely by the macrophage-dependent efferocytotic pathway (Weiss et al., 2019). However, our data support the hypothesis that the

chemokine secretome of metabolically fit MSCs not otherwise deployed by dead cells provides a biologically plausible mechanism of action for MSCs in DSS colitis and by extension to any acute tissue injury syndrome where CCL2/CXCL12-driven M2 polarization of tissue-resident macrophages is desirable to affect outcomes.

STAR★METHODS

LEAD CONTACT AND MATERIALS AVAILABILITY

Please direct all requests for reagents and resources to the lead contact: Jacques Galipeau (jgalipeau@wisc.edu). This study did not produce new unique reagents.

EXPERIMENTAL MODEL AND SUBJECT DETAILS

Animals—C57BL/6, B6.129P2-IL-10tm1cgn/J and B6.129S4-Ccl2tm1Rol/J, B6(Cg)-IL-10tm1.1Karp/J (Vert-X) female mice were all age-matched (3–6 months old) and purchased from the Jackson Laboratory (Bar Harbor, ME). All animal experiments were approved by the University of Wisconsin-Madison Institutional Animal Care and Use Committee and performed in accordance with the Animal Care and Use Policies at the University of Wisconsin as described previously (Djamali et al., 2005, 2009).

Isolation and expansion of bone marrow MSC—Bone marrow MSCs were collected by flushing the femurs and tibiae of 3–6-months old C57BL/6 mice in aseptic conditions, and cultured with complete media (DMEM, 10% FBS) supplemented with penicillin and streptomycin (Lonza). After 3 day of culture non-adherent hematopoietic cells were removed by changing the medium. Whole medium was subsequently changed every 3–4 days until nearly confluent. Adherent cells were then detached by 0.25% trypsin-EDTA and reseeded at a density of 5,000/cm^2. Thereafter, the cells were passaged weekly with changing the medium every 3–4 days. After the third passage, the MSC cultures were assayed by flow cytometric analysis and used in the experiments at passage 3 and 5. For IFNγ priming, MSCs were seeded with the complete media containing mouse recombinant IFNγ (R&D) at a concentration of 25 ng/ml for 48 h.

Isolation and culture of peritoneal cavity derived macrophages—To isolate peritoneal cavity derived macrophages, wild-type (WT) or IL-$10^{-/-}$ C57BL/6 mice were injected 5 mL of ice cold PBS (with 3% FCS) into the peritoneal cavity followed by gentle massaging of the abdomen. The PBS solution was retrieved and after centrifugation at 300 g x 5min cells were seeded in complete RPMI medium containing 10% heat inactivated FBS, supplemented with penicillin and streptomycin. After 24 h non-adherent cells were washed out and cells were detached from the plate using accutase solution (Corning) and ready for performing assays.

METHOD DETAILS

Colitis induction and experimental design—Colitis was induced in 3–6-months-old female C57BL/6 mice or IL-$10^{-/-}$ mice by administering 4% (w/v) DSS (molecular weight: 36,000 to 50,000 Da; MP Biochemicals, Santa Ana, CA, USA) via drinking water for 6 days and normal drinking water afterward. BM-MSCs (1×10^7 cells/ml) were injected

intraperitoneally into the DSS treated mice (N = 5) on days 2 and 4 (BM-MSC-treated group). Dosage and frequency of BM-MSCs were ascertained on the basis of our preliminary data and previous studies (Song et al., 2017a). The therapeutic effect of BM-MSC treatment was assessed by clinicopathologic measurements of body weight, Disease Activity scoring (DAI) scoring, and histological scoring. During the duration of the experiment, a disease activity index (DAI) score was evaluated to assess the clinical progression of colitis as described previously (Yang et al., 2018).

Preparation of conditioned medium from cultured MSCs—MSCs were grown as mentioned above. Once cells reached confluency, the conditioned media was collected from the same passage (Passage 4) centrifuged at 1500 rpm for 5 min, filtered, and used for treatment. For generating IFNγ primed MSC condition media the cells were kept with fresh complete media for 24h after removal of IFNγ containing medium and the following day processed the medium as mentioned above to perform the assays.

Histological analysis—Colonic segments were stained with hematoxylin and eosin (H&E) and colitis severity was assessed based on the following parameters as described (Alex et al., 2009): (1) epithelial damage (0: none; 1: minimal loss of goblet cells; 2: massive loss of goblet cells; 3: slight loss of crypts; and 4: massive loss of crypts), and (2) infiltration (0: none; 1: crypt base infiltration; 2: mucosa infiltration; 3: severe mucosa infiltration and edema; and 4: submucosa infiltration). Histological activity index (HAI) ranging from 0 (unaffected) to 8 (severe colitis) was estimated as the sum of the epithelium and infiltration score. Images were taken by optical microscope (ZEISS Vert. A1).

Enzyme-Linked Immunosorbent Assay—CCL2 concentration in the MSC condition media was evaluated using CCL2 ELISA kit (Invitrogen) following manufacturer's instructions. For detecting IL-10, PMϕ were treated with MSC-CM for 24h, the supernatant was collected on following day and amount of IL-10 was measured using IL-10 ELISA kit (Invitrogen) following manufacturer's instructions.

Flow cytometry analysis—Flow cytometry was performed on Attune NxT Flow Cytometer (Thermo Fisher Scientific) using fluorochrome conjugated mAbs with corresponding isotype matched controls. Live/dead cell separation was done by staining cells with Ghost red 780 viability dye (Tonbo bioscience). 1X PBS containing 0.5% BSA and 0.05% Azide use consistently as FACS buffer for incubating cells with antibodies, and for washing. For intracellular staining of iNOS and Ki67, intracellular staining kit (BD Bioscience) was used, following the manufacturer's instructions. Flow data were analyzed using FCS Express 6 flow cytometry software.

T cell proliferation assay—Spleens were harvested from C57BL/6 mice and kept on a cell strainer. Using the plunger end of a 1 mL syringe, the spleen was mashed through the cell strainer into a 50 mL falcon tube. After centrifugation, red blood cells were lysed using RBC lysis buffer (Lonza). T cells were isolated by negative selection (STEMCELL technologies) as per manufacturer protocol. Isolated T cells were stimulated with anti-CD3/CD28 DynaBeads (GIBCO, life technologies) and cocultured with MSC-CM pretreated

PMϕ at a ratio of 2:1, for 72 h. Flow cytometry study was performed to detect T cell proliferation by measuring CD3 and Ki67 dual positive population.

Preparation of concentrated MSC-CM—To prepare concentrated MSC-CM, MSC supernantant was collected and filtered to remove cell debris and the supernatant was concentrated using an Amicon Ultra centrifugal filter of 3kDa cut off column (MilliporeSigma, Burlington, MA, USA). To prevent protein degradation, protease inhibitors were added into the newly generated concentrated media. For immunoprecipitation study 20x concentrated conditioned media was used.

Immunoprecipitation and immunoblotting—To immunoprecipitate concentrated media, pierce magnetic beads were used and the manufacturer's instructions were followed. Briefly, to maintain the intact binding of proteins, the concentrated MSC-CM was incubated with EGS [ethylene glycol-bis(succinimidylsuccinate)] for 2 h in ice. The cross-linking reaction was stopped by adding Tris-HCl, pH 7.4 for 15 min followed by overnight incubation with the antibodies in a rotating platform at 4°C. The following day, media was incubated with precleared magnetic beads for 3–4 h in rotating platform at 4°C. Beads were collected, washed 3x and the immunoprecipitated samples were eluted using either 2X laemmili buffer (for western blot) or 0.1M glycine (for chemokine array) followed by neutralizing the solution with 1M tris, pH 8.5.

Total protein eluted were resolved by 10% SDS-PAGE and blotted to nitrocellulose membrane (Millipore, Billerica, MA). Membranes were then probed with primary Ab overnight at the dilution recommended by the suppliers followed by incubation with secondary antibody for 1 hour at room temperature. Chemiluminescence was identified using clarity™ Western ECL Substrate (BioRad).

Chemokine array—Chemokine array was performed with immunoprecipitated concentrated MSC-CM using Proteome Profiler Mouse Chemokine Array Kit (R&D system, ARY020) following the manufacturer's instructions.

Isolation of leukocytes from intestinal intraepithelial layer and lamina propria —Small bowel (jejunum and ileum) and large bowel (cecum and colon) were carefully detached, and mesentery and fat were removed. Feces were washed out, and Peyer's patches were removed from the small intestine. Leukocytes were isolated as described previously (Couter and Surana, 2016). Briefly, bowel sections were cut and incubated in prewarmed extraction media with a constant stirring at 500 rpm at 37°C. For digesting the tissues, tissue pieces were digested in dispase, collagenase II and 2% FBS containing RPMI media. After repeated washing followed by digestion, pellet was resuspended in flow cytometry staining buffer and proceed for flow study as mentioned above.

QUANTIFICATION AND STATISTICAL ANALYSIS

The number of biological and technical replicates and the number of animals are mentioned in figure legends and text. Statistical data were generated using GraphPad Prism 5.0 software. For all experiments with error bars, the standard error of the mean (SEM) was estimated to specify the variation within each experiment. An unpaired two-sided t test was

used to identify significance between the means of two groups, while a one/Two-way ANOVA using Tukey's Multiple Comparison Test was used to compare multiple groups simultaneously. Statistical significance was defined as a Two-sided p value < 0.05.

DATA AND CODE AVAILABILITY

This study did not generate/analyze datasets/code.

Supplementary Material

Refer to Web version on PubMed Central for supplementary material.

ACKNOWLEDGMENTS

This work was supported by National Institutes of Health, National Institute of Diabetes and Digestive and Kidney Diseases award R01DK109508 to J. Galipeau. This study was also supported by University of Wisconsin Carbone Cancer Center support grant P30 CA014520. We thank lab members of the Galipeau Lab for comments and suggestions on the manuscripts and T. Kinoshita for assistance in sectioning the colon tissue and H&E staining.

REFERENCES

Alex P, Zachos NC, Nguyen T, Gonzales L, Chen T-E, Conklin LS, Centola M, and Li X (2009). Distinct cytokine patterns identified from multiplex profiles of murine DSS and TNBS-induced colitis. Inflamm. Bowel Dis 15, 341–352. [PubMed: 18942757]

Asada N, Kunisaki Y, Pierce H, Wang Z, Fernandez NF, Birbrair A, Ma'ayan A, and Frenette PS (2017). Differential cytokine contributions of perivascular haematopoietic stem cell niches. Nat. Cell Biol 19, 214–223. [PubMed: 28218906]

Braid LR, Wood CA, Wiese DM, and Ford BN (2018). Intramuscular administration potentiates extended dwell time of mesenchymal stromal cells compared to other routes. Cytotherapy 20, 232–244. [PubMed: 29167063]

Caplan H, Olson SD, Kumar A, George M, Prabhakara KS, Wenzel P, Bedi S, Toledano-Furman NE, Triolo F, Kamhieh-Milz J, et al. (2019). Mesenchymal Stromal Cell Therapeutic Delivery: Translational Challenges to Clinical Application. Front. Immunol 10, 1645. [PubMed: 31417542]

Chinnadurai R, Ng S, Velu V, and Galipeau J (2015). Challenges in animal modelling of mesenchymal stromal cell therapy for inflammatory bowel disease. World J. Gastroenterol 21, 4779–4787. [PubMed: 25944991]

Chinnadurai R, Rajan D, Qayed M, Arafat D, Garcia M, Liu Y, Kugathasan S, Anderson LJ, Gibson G, and Galipeau J (2018). Potency Analysis of Mesenchymal Stromal Cells Using a Combinatorial Assay Matrix Approach. Cell Rep. 22, 2504–2517. [PubMed: 29490284]

Chiossone L, Conte R, Spaggiari GM, Serra M, Romei C, Bellora F, Becchetti F, Andaloro A, Moretta L, and Bottino C (2016). Mesenchymal Stromal Cells Induce Peculiar Alternatively Activated Macrophages Capable of Dampening Both Innate and Adaptive Immune Responses. Stem Cells 34, 1909–1921. [PubMed: 27015881]

Cho D-I, Kim MR, Jeong HY, Jeong HC, Jeong MH, Yoon SH, Kim YS, and Ahn Y (2014). Mesenchymal stem cells reciprocally regulate the M1/M2 balance in mouse bone marrow-derived macrophages. Exp. Mol. Med 46, e70. [PubMed: 24406319]

Ciccocioppo R, Baumgart DC, Dos Santos CC, Galipeau J, Klersy C, and Orlando G (2019). Perspectives of the International Society for Cell & Gene Therapy Gastrointestinal Scientific Committee on the Intravenous Use of Mesenchymal Stromal Cells in Inflammatory Bowel Disease (PeMeGi). Cytotherapy 21, 824–839. [PubMed: 31201092]

Couter CJ, and Surana NK (2016). Isolation and Flow Cytometric Characterization of Murine Small Intestinal Lymphocytes. J. Vis. Exp 111, 10.3791/54114.

Djamali A, Reese S, Oberley T, Hullett D, and Becker B (2005). Heat shock protein 27 in chronic allograft nephropathy: a local stress response. Transplantation 79, 1645–1657. [PubMed: 15973165]

Djamali A, Vidyasagar A, Adulla M, Hullett D, and Reese S (2009). Nox-2 is a modulator of fibrogenesis in kidney allografts. Am. J. Transplant 9, 74–82. [PubMed: 18976289]

Duijvestein M, Wildenberg ME, Welling MM, Hennink S, Molendijk I, van Zuylen VL, Bosse T, Vos ACW, de Jonge-Muller ESM, Roelofs H, et al. (2011). Pretreatment with interferon-γ enhances the therapeutic activity of mesenchymal stromal cells in animal models of colitis. Stem Cells 29, 1549–1558. [PubMed: 21898680]

Dyer DP, Salanga CL, Johns SC, Valdambrini E, Fuster MM, Milner CM, Day AJ, and Handel TM (2016). The Anti-inflammatory Protein TSG-6 Regulates Chemokine Function by Inhibiting Chemokine/Glycosaminoglycan Interactions. J. Biol. Chem 291, 12627–12640. [PubMed: 27044744]

Farahani RM, and Xaymardan M (2015). Platelet-Derived Growth Factor Receptor Alpha as a Marker of Mesenchymal Stem Cells in Development and Stem Cell Biology. Stem Cells Int. 2015, 362753. [PubMed: 26257789]

Galipeau J, and Sensébé L (2018). Mesenchymal Stromal Cells: Clinical Challenges and Therapeutic Opportunities. Cell Stem Cell 22, 824–833. [PubMed: 29859173]

Galleu A, Riffo-Vasquez Y, Trento C, Lomas C, Dolcetti L, Cheung TS, von Bonin M, Barbieri L, Halai K, Ward S, et al. (2017). Apoptosis in mesenchymal stromal cells induces *in vivo* recipient-mediated immunomodulation. Sci. Transl. Med 9, 9.

Ghazanfari R, Li H, Zacharaki D, Lim HC, and Scheding S (2016). Human Non-Hematopoietic CD271pos/CD140alow/neg Bone Marrow Stroma Cells Fulfill Stringent Stem Cell Criteria in Serial Transplantations. Stem Cells Dev. 25, 1652–1658. [PubMed: 27527928]

Gouwy M, Struyf S, Noppen S, Schutyser E, Springael J-Y, Parmentier M, Proost P, and Van Damme J (2008). Synergy between coproduced CC and CXC chemokines in monocyte chemotaxis through receptor-mediated events. Mol. Pharmacol 74, 485–495. [PubMed: 18469140]

Grégoire C, Lechanteur C, Briquet A, Baudoux É, Baron F, Louis E, and Beguin Y (2017). Review article: mesenchymal stromal cell therapy for inflammatory bowel diseases. Aliment. Pharmacol. Ther 45, 205–221. [PubMed: 27878827]

Hidalgo-Garcia L, Galvez J, Rodriguez-Cabezas ME, and Anderson PO (2018). Can a Conversation Between Mesenchymal Stromal Cells and Macrophages Solve the Crisis in the Inflamed Intestine? Front. Pharmacol. 9, 179. [PubMed: 29559912]

Ho IAW, Chan KYW, Ng W-H, Guo CM, Hui KM, Cheang P, and Lam PYP (2009). Matrix metalloproteinase 1 is necessary for the migration of human bone marrow-derived mesenchymal stem cells toward human glioma. Stem Cells 27, 1366–1375. [PubMed: 19489099]

Ho IAW, Yulyana Y, Sia KC, Newman JP, Guo CM, Hui KM, and Lam PYP (2014). Matrix metalloproteinase-1-mediated mesenchymal stem cell tumor tropism is dependent on crosstalk with stromal derived growth factor 1/C-X-C chemokine receptor 4 axis. FASEB J. 28, 4359–4368. [PubMed: 25271298]

Hoogduijn MJ, and Lombardo E (2019). Mesenchymal Stromal Cells Anno 2019: Dawn of the Therapeutic Era? Concise Review. Stem Cells Transl. Med 8, 1126–1134. [PubMed: 31282113]

Hughes CE, and Nibbs RJB (2018). A guide to chemokines and their receptors. FEBS J. 285, 2944–2971. [PubMed: 29637711]

Karpova D, and Bonig H (2015). Concise Review: CXCR4/CXCL12 Signaling in Immature Hematopoiesis-Lessons From Pharmacological and Genetic Models. Stem Cells 33, 2391–2399. [PubMed: 25966814]

Lee HK, Kim HS, Kim JS, Kim YG, Park KH, Lee JH, Kim KH, Chang IY, Bae S-C, Kim Y, et al. (2017). CCL2 deficient mesenchymal stem cells fail to establish long-lasting contact with T cells and no longer ameliorate lupus symptoms. Sci. Rep 7, 41258. [PubMed: 28117437]

Li B, Alli R, Vogel P, and Geiger TL (2014). IL-10 modulates DSS-induced colitis through a macrophage-ROS-NO axis. Mucosal Immunol. 7, 869–878. [PubMed: 24301657]

Madan R, Demircik F, Surianarayanan S, Allen JL, Divanovic S, Trompette A, Yogev N, Gu Y, Khodoun M, Hildeman D, et al. (2009). Nonredundant roles for B cell-derived IL-10 in immune counter-regulation. J. Immunol 183, 2312–2320. [PubMed: 19620304]

Mantovani A, Sica A, Sozzani S, Allavena P, Vecchi A, and Locati M (2004). The chemokine system in diverse forms of macrophage activation and polarization. Trends Immunol. 25, 677–686. [PubMed: 15530839]

Matsuzaki Y, Mabuchi Y, and Okano H (2014). Leptin receptor makes its mark on MSCs. Cell Stem Cell 15, 112–114. [PubMed: 25105573]

Melief SM, Schrama E, Brugman MH, Tiemessen MM, Hoogduijn MJ, Fibbe WE, and Roelofs H (2013). Multipotent stromal cells induce human regulatory T cells through a novel pathway involving skewing of monocytes toward anti-inflammatory macrophages. Stem Cells 31, 1980–1991. [PubMed: 23712682]

Miller MC, and Mayo KH (2017). Chemokines from a Structural Perspective. Int. J. Mol. Sci 18, 18.

Moll G, Ankrum JA, Kamhieh-Milz J, Bieback K, Ringdén O, Volk H-D, Geissler S, and Reinke P (2019). Intravascular Mesenchymal Stromal/Stem Cell Therapy Product Diversification: Time for New Clinical Guidelines. Trends Mol. Med 25, 149–163. [PubMed: 30711482]

Müller E, Christopoulos PF, Halder S, Lunde A, Beraki K, Speth M, Øynebråten I, and Corthay A (2017). Toll-Like Receptor Ligands and Interferon-γ Synergize for Induction of Antitumor M1 Macrophages. Front. Immunol 8, 1383. [PubMed: 29123526]

Németh K, Leelahavanichkul A, Yuen PST, Mayer B, Parmelee A, Doi K, Robey PG, Leelahavanichkul K, Koller BH, Brown JM, et al. (2009). Bone marrow stromal cells attenuate sepsis via prostaglandin E(2)-dependent reprogramming of host macrophages to increase their interleukin-10 production. Nat. Med 15, 42–49. [PubMed: 19098906]

Nesmelova IV, Sham Y, Gao J, and Mayo KH (2008). CXC and CC chemokines form mixed heterodimers: association free energies from molecular dynamics simulations and experimental correlations. J. Biol. Chem 283, 24155–24166. [PubMed: 18550532]

Panés J, García-Olmo D, Van Assche G, Colombel JF, Reinisch W, Baumgart DC, Dignass A, Nachury M, Ferrante M, Kazemi-Shirazi L, et al.; ADMIRE CD Study Group Collaborators (2016). Expanded allogeneic adipose-derived mesenchymal stem cells (Cx601) for complex perianal fistulas in Crohn's disease: a phase 3 randomised, double-blind controlled trial. Lancet 388, 1281–1290. [PubMed: 27477896]

Panés J, Garcia-Olmo D, Van Assche G, Colombel JF, Reinisch W, Baumgart DC, Dignass A, Nachury M, Ferrante M, Kazemi-Shirazi L, et al. (2018a). Long-term Efficacy and Safety of Stem Cell Therapy (Cx601) for Complex Perianal Fistulas in Patients With Crohn's Disease. Gastroenterology 154, 1334–1342.e1334. [PubMed: 29277560]

Panes J, García-Olmo D, Van Assche G, Colombel JF, Reinisch W, Baumgart DC, Dignass A, Nachury M, Ferrante M, Kazemi-Shirazi L, et al.; ADMIRE CD Study Group Collaborators (2018b). Long-term Efficacy and Safety of Stem Cell Therapy (Cx601) for Complex Perianal Fistulas in Patients With Crohn's Disease. Gastroenterology 154, 1334–1342.e4. [PubMed: 29277560]

Proudfoot AEI, and Uguccioni M (2016). Modulation of Chemokine Responses: Synergy and Cooperativity. Front. Immunol 7, 183. [PubMed: 27242790]

Rafei M, Hsieh J, Fortier S, Li M, Yuan S, Birman E, Forner K, Boivin M-N, Doody K, Tremblay M, et al. (2008). Mesenchymal stromal cell-derived CCL2 suppresses plasma cell immunoglobulin production via STAT3 inactivation and PAX5 induction. Blood 112, 4991–998. [PubMed: 18812467]

Rafei M, Campeau PM, Aguilar-Mahecha A, Buchanan M, Williams P, Birman E, Yuan S, Young YK, Boivin M-N, Forner K, et al. (2009). Mesenchymal stromal cells ameliorate experimental autoimmune encephalomyelitis by inhibiting CD4 Th17 T cells in a CC chemokine ligand 2-dependent manner. J. Immunol 182, 5994–6002. [PubMed: 19414750]

Roca H, Varsos ZS, Sud S, Craig MJ, Ying C, and Pienta KJ (2009). CCL2 and interleukin-6 promote survival of human CD11b+ peripheral blood mononuclear cells and induce M2-type macrophage polarization. J. Biol. Chem 284, 34342–34354. [PubMed: 19833726]

Sala E, Genua M, Petti L, Anselmo A, Arena V, Cibella J, Zanotti L, D'Alessio S, Scaldaferri F, Luca G, et al. (2015). Mesenchymal Stem Cells Reduce Colitis in Mice via Release of TSG6,

Independently of Their Localization to the Intestine. Gastroenterology 149, 163–176.e20. [PubMed: 25790743]

Sheridan C (2018). First off-the-shelf mesenchymal stem cell therapy nears European approval. Nat. Biotechnol. 36, 212–214.

Shi C, Jia T, Mendez-Ferrer S, Hohl TM, Serbina NV, Lipuma L, Leiner I, Li MO, Frenette PS, and Pamer EG (2011). Bone marrow mesenchymal stem and progenitor cells induce monocyte emigration in response to circulating toll-like receptor ligands. Immunity 34, 590–601. [PubMed: 21458307]

Shi Y, Wang Y, Li Q, Liu K, Hou J, Shao C, and Wang Y (2018). Immunoregulatory mechanisms of mesenchymal stem and stromal cells in inflammatory diseases. Nat. Rev. Nephrol 14, 493–507. [PubMed: 29895977]

Song J-Y, Kang HJ, Hong JS, Kim CJ, Shim J-Y, Lee CW, and Choi J (2017a). Umbilical cord-derived mesenchymal stem cell extracts reduce colitis in mice by re-polarizing intestinal macrophages. Sci. Rep 7, 9412. [PubMed: 28842625]

Song W-J, Li Q, Ryu M-O, Ahn J-O, Ha Bhang D, Chan Jung Y, and Youn H-Y (2017b). TSG-6 Secreted by Human Adipose Tissue-derived Mesenchymal Stem Cells Ameliorates DSS-induced colitis by Inducing M2 Macrophage Polarization in Mice. Sci. Rep 7, 5187. [PubMed: 28701721]

Takeda K, Webb TL, Ning F, Shiraishi Y, Regan DP, Chow L, Smith MJ, Ashino S, Guth AM, Hopkins S, et al. (2018). Mesenchymal Stem Cells Recruit CCR2^{+} Monocytes To Suppress Allergic Airway Inflammation. J. Immunol 200, 1261–1269. [PubMed: 29352000]

Tikhonova AN, Dolgalev I, Hu H, Sivaraj KK, Hoxha E, Cuesta-Domínguez Á, Pinho S, Akhmetzyanova I, Gao J, Witkowski M, et al. (2019). The bone marrow microenvironment at single-cell resolution. Nature 569, 222–228. [PubMed: 30971824]

Varol C, Mildner A, and Jung S (2015). Macrophages: development and tissue specialization. Annu. Rev. Immunol 33, 643–675. [PubMed: 25861979]

Vasandan AB, Jahnavi S, Shashank C, Prasad P, Kumar A, and Prasanna SJ (2016). Human Mesenchymal stem cells program macrophage plasticity by altering their metabolic status via a PGE2-dependent mechanism. Sci. Rep 6, 38308. [PubMed: 27910911]

Weiss DJ, English K, Krasnodembskaya A, Isaza-Correa JM, Hawthorne IJ, and Mahon BP (2019). The Necrobiology of Mesenchymal Stromal Cells Affects Therapeutic Efficacy. Front. Immunol 10, 1228. [PubMed: 31214185]

Yang FY, Chen R, Zhang X, Huang B, Tsang LL, Li X, and Jiang X (2018). Preconditioning Enhances the Therapeutic Effects of Mesenchymal Stem Cells on Colitis Through PGE2-Mediated T-Cell Modulation. Cell Transplant. 27, 1352–1367. [PubMed: 30095002]

Highlights

- Host macrophages (Mϕ) are indispensable for BM-MSC-dependent reduction of colitis
- MSC-secreted chemokines CCL2 and CXCL12 synergistically induce M2 polarization
- Host IL-10 competency is crucial for MSC-mediated recovery of DSS colitis
- MSC-polarized host Mϕ regulate IL-10 polarization by gut-bound lymphoid cells

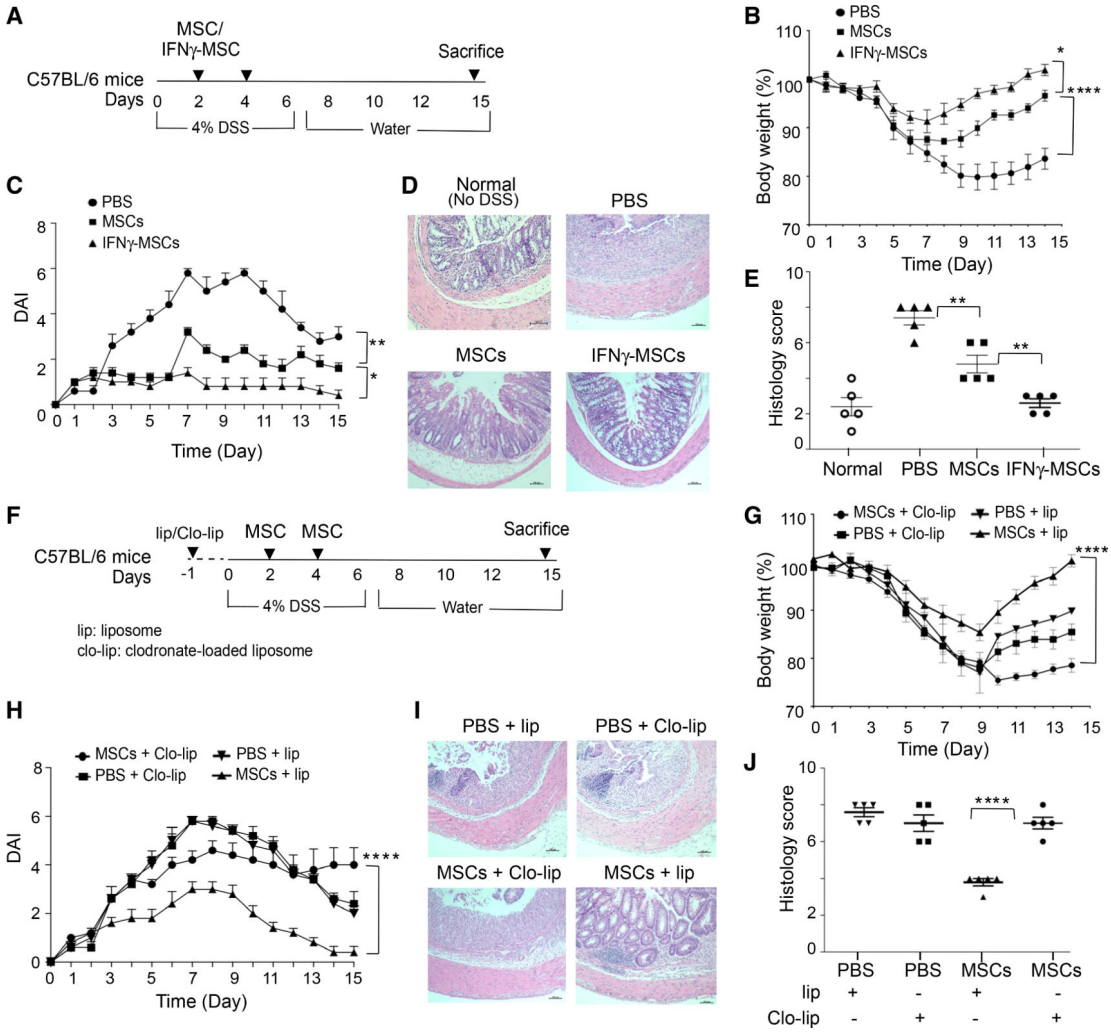

Figure 1. Clodronate-Sensitive Macrophages Are Essential for the Therapeutic Effect of Intraperitoneal-Delivered BM-MSCs in DSS-Induced Colitis

(A) Schematic of the experimental setup for results shown in (B)–(E).

(F) Schematic of the experimental setup for results shown in (G)–(J) (mice, n = 5 per test group).

B6 mice were administered an intravenous injection of clodronate-loaded liposome (Clo-lip) of 50 mg kg^{-1} 24 h before DSS treatment; liposome vehicle (lip) served as a control. For IFNγ prelicensing, MSCs were treated with 25 ng/ml IFNγ for 48 h (A–E). Development of colitis was monitored by measuring body weight change relative to the initial body weight at day 0 (in B and G), disease activity index (in C and H), H&E staining of colon (in D and I), and histological score (in E and J). Scale bars in (D) and (I) represent 100 μm. Statistical analysis was performed by Student's t test for (E) and (J); two-way ANOVA (Tukey test) for rest of all experiments; *$p < 0.05$, **$p < 0.01$, ***$p < 0.001$, ****$p < 0.0001$.

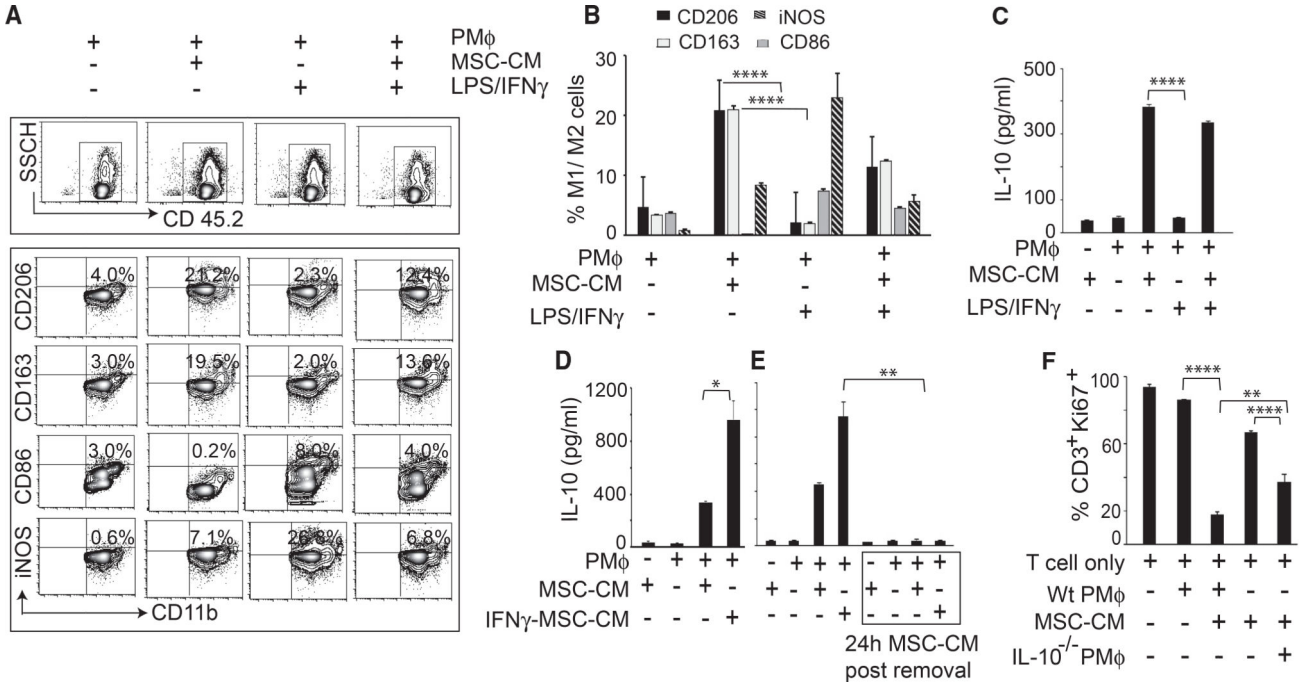

Figure 2. BM-MSC Secretome Induces Peritoneal Macrophage M2 Polarization That Is Functionally Dependent on IL-10 Expression for Bystander T Cell Suppression

(A) Diagram shows representative plots for flow cytometric analysis of the peritoneal-cavity-derived macrophages (PMϕ). Expression of M1-specific surface markers CD86 and CD163 and M2-specific surface markers CD206 and CD163 on CD45.2 (top panel) and CD11b (bottom panel) double-positive cells are shown in overnight MSC-CM-treated PMϕ.

(B) Quantification shows percentages of M1 or M2 cells from experiments in (A).

(C) IL-10 released in the supernatants of MSC-CM-treated macrophages was quantified using ELISA. LPS/IFNγ-treated macrophages served as a control.

(D) IL-10 released in the supernatants of the IFNγ-primed MSC-CM-treated macrophages was quantified using ELISA.

(E) PMϕ were treated with MSC-CM and IFNγ-pretreated MSC-CM overnight; the day after, MSC-CM was replaced with fresh PMϕ media. IL-10 released in the supernatants of macrophages was quantified by ELISA.

(F) Splenic T cells were cultured with MSC-CM alone, MSC-CM-treated naive PMϕ, or IL-$10^{-/-}$ PMϕ for 72 h. T cell proliferation was assessed by Ki67 intracellular staining.

Statistical analysis was performed by Student's t test for (A)–(E) and one-way ANOVA (Tukey test) for (F); *$p < 0.05$, **$p < 0.01$, ***$p < 0.001$, ****$p < 0.0001$.

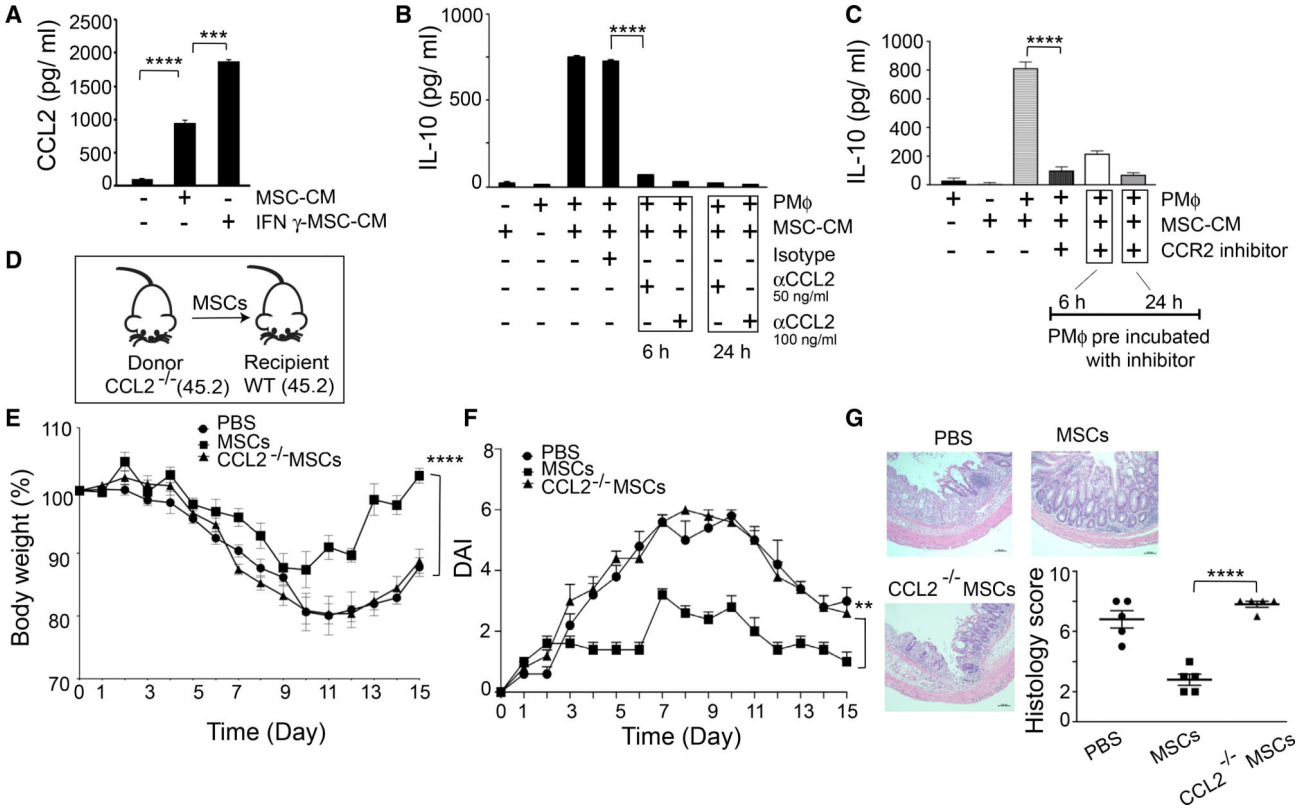

Figure 3. BM-MSC-Derived CCL2 Induces Macrophage M2 Polarization

(A) CCL2 released in the supernatant of MSCs alone or IFNγ-pretreated MSCs were measured by ELISA.

(B) IL-10 released in the supernatants of PMϕ cultured with MSC-CM (with/out CCL2 antibody treatment) was quantified using ELISA, at the indicated time points.

(C) Released IL-10 was quantified in the supernatant of PMϕ using ELISA. Here in one set of experiments, PMϕ was co-incubated with MSC-CM and CCR2 antagonist RS 102895. In another set, CCR2 antagonist pretreatment of PMϕ was performed at indicated time points followed by overnight incubation with MSC-CM.

(D) Cartoon shows the experimental schemes for results described in (E)–(G). Mice (n = 5 per test group) received 4.0% (w/v) of DSS orally for 6 days. MSC derived from bone marrow of $CCL2^{-/-}$ mice was transferred intraperitoneally (i.p.) into the mice at days 2 and 4.

(E–G) Development of colitis was monitored by measuring body weight change relative to the initial body weight at day 0 (E), disease activity index (F), and H&E staining of colon and histological score (G).

Error bars represent the mean ± SEM (n = 3 for A–C and n = 5 for E–G). Scale bars in (G) represent 100 μm. Statistical analysis was performed by Student's t test for (A)-(C) and (G) and two-way ANOVA (Tukey test) for (E) and (F); **p < 0.01, ***p <0.001, ****p < 0.0001.

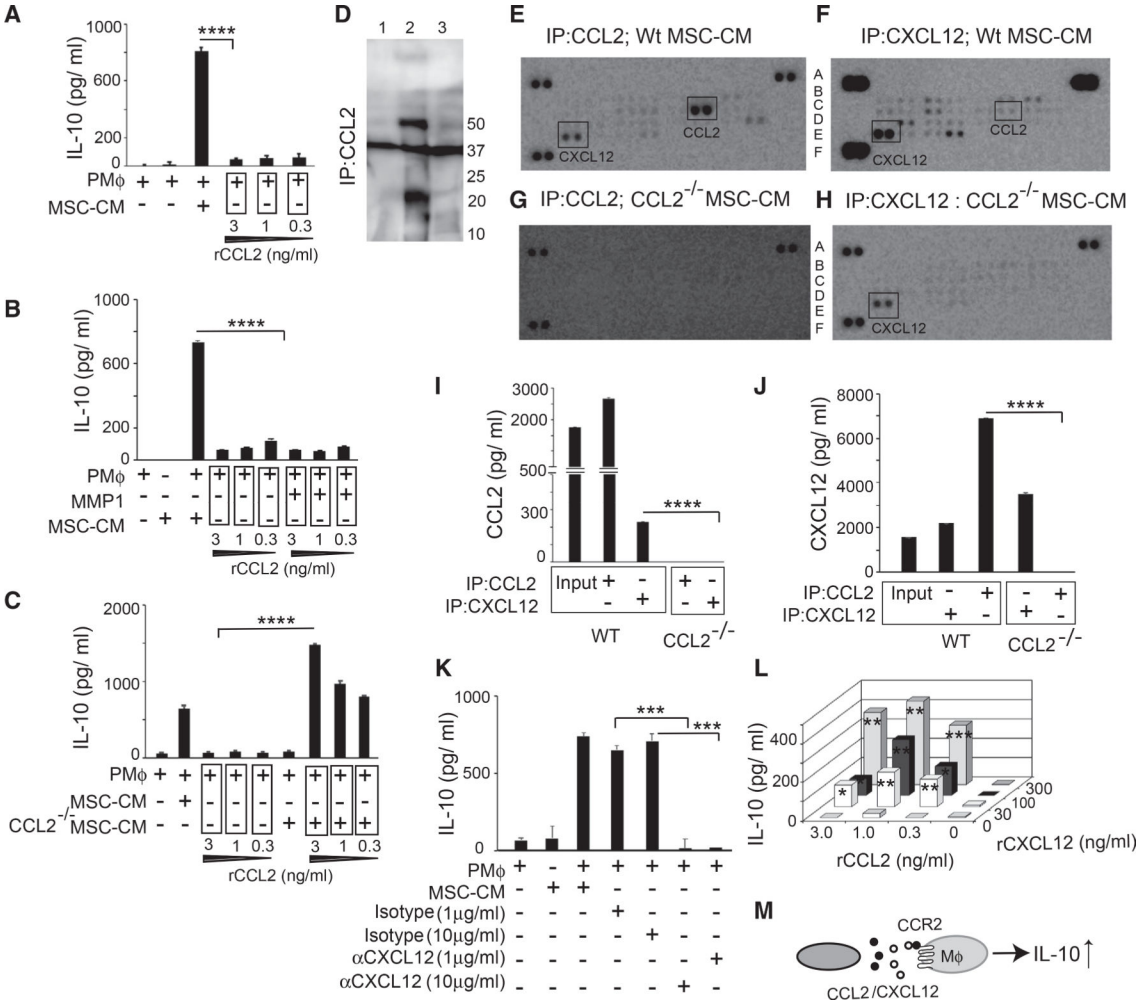

Figure 4. MSC-Secreted Chemokines CCL2 and CXCL12 Synergistically Induce Macrophage M2 Polarization

(A–C) PMϕ were treated with rCCL2 alone (A), with rCCL2 plus MMP1 (B), and rCCL2 plus CCL2$^{-/-}$ MSC-CM (C). MSC-CM-treated PMϕ served as a positive control. The concentrations of rCCL2 used in those experiments were 0.3, 1.0, and 3.0 ng/ml. IL-10 expression was assessed by ELISA (A–C).

(D) Western blot of immunoprecipitated CCL2 from MSC-CM; lane 1, no antibody control; lane 2, with cross-linker EGS; and lane 3, without cross-linker.

(E–H) Mouse-specific chemokine protein array was performed with wild-type (WT) MSC-CM (E and F) and CCL2$^{-/-}$ MSC-CM (G and H). Immunoprecipitations were performed using CCL2- (E and G) and CXCL12- (F and H) specific antibodies.

(I) CCL2 expression was assessed by ELISA under indicated conditions.

(J) CXCL12 expression was assessed by ELISA under indicated conditions.

(K) IL-10 released in the supernatants of PMϕ cultured with MSC-CM (with/out CXCL12 antibody treatment at the indicated concentrations) was quantified using ELISA. Isotype-treated cells served as negative control.

(L) IL-10 release in the supernatants of PMϕ was assessed using ELISA. PMϕ were cultured with/out rCCL2 and rCXCL12 at indicated concentrations.

(M) Cartoon demonstrates the synergistic action of CCL2 and CXCL12 on PMϕ to induce IL-10 production.

Average ± SEM of triplicate repeats are shown. *p < 0.05, **p < 0.01, ***p < 0.001, ****p < 0.0001 by Student's t test.

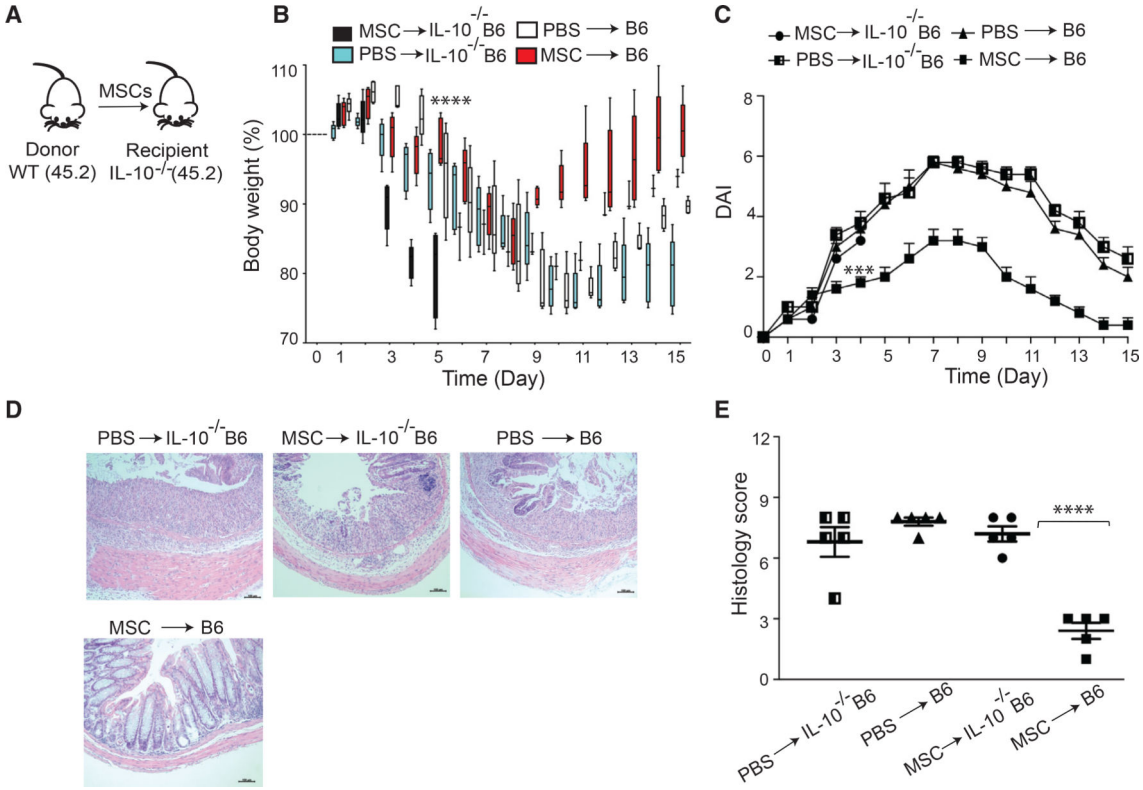

Figure 5. Host IL-10 Competency Is Indispensable for MSC-Mediated Recovery of DSS Colitis

(A) Cartoon shows the experimental schemes for results described in (B)–(E). Mice (n = 5 per test group) received 4.0% (w/v) of DSS orally for 6 days. MSC was transferred i.p. into the syngeneic IL-10$^{-/-}$ mice at days 2 and 4.

(B-E) The development of colitis is monitored by measuring body weight change relative to the initial body weight at day 0 (B), disease activity index (C), H&E staining (D), and histological score (E). MSC transfusion (i.p.) into B6 mice served as positive control. Error bars represent the mean ± SEM (n = 5 for all experiments). Scale bars in (D) represent 100 μm. Statistical analysis was performed by Student's t test for (E) and by two-way ANOVA for (B) and (C) (Tukey test); ***p < 0.001, ****p < 0.0001.

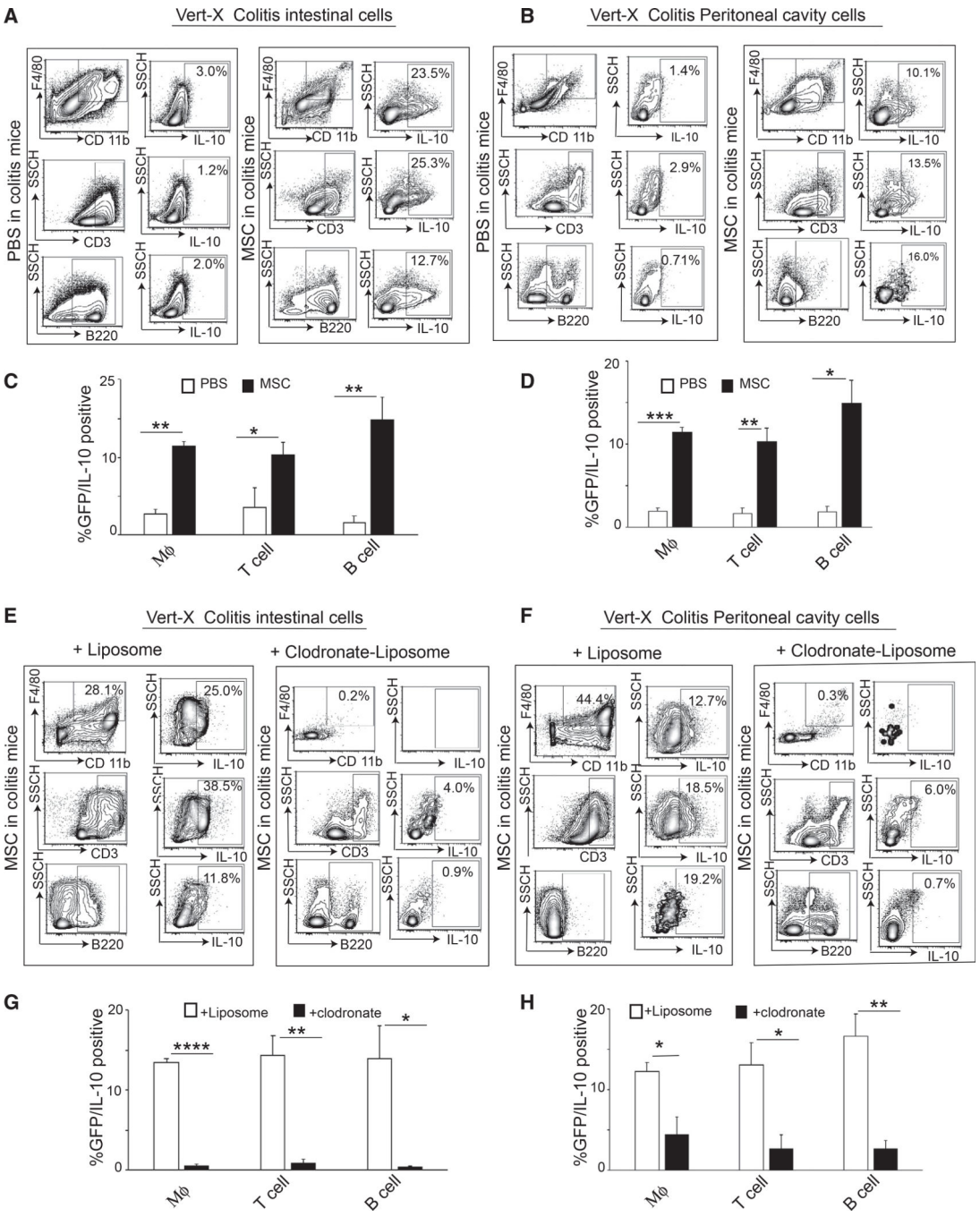

Figure 6. BM-MSC-Polarized Host Macrophages Secondarily Mobilize IL-10$^+$ Gut- and Tissue-Resident T and B Cells

(A–H) IL-10 expression was monitored in MSC-injected colitic mice (n = 3) in the presence (A–D) and absence (E–H) of macrophages.

(A–D) Intestinal (A and C) and peritoneal cavity (B and D) cells were stained with specific markers for macrophages (CD 11b and F4/80), T cell (CD3), and B cell (B220); GFP-positive cells were analyzed as a surrogate of IL-10 expression.

The cumulative data of three experiments of (A) and (B) were shown in (C) and (D), respectively, as well as the cumulative data of three experiments of (E) and (F) were shown

in (G) and (H), respectively. *p < 0.05; **p < 0.01, ***p < 0.001, ****p < 0.0001 by Student's t test.

KEY RESOURCES TABLE

REAGENT or RESOURCE	SOURCE	IDENTIFIER
Antibodies		
Armenian Hamster anti MCP-1	Abcam	Cat # ab21396, RRID:AB_446255
Rabbit anti MCP-1	Cell signaling Technologies	Cat # 2029, RRID:AB_1264199
Rabbit anti CXCL12	Thermo Fisher Scientific	Cat # PA1-29029, RRID:AB_2276940
Anti-Mouse CD 45.2 APC	BD PharMingen	Cat # 558702, RRID:AB_1645215
Anti-Mouse CD11b PE	BD PharMingen	Cat # 557397, RRID:AB_396680
Anti-Mouse CD206 PE	Biolegend	Cat # 141706, RRID:AB_10895754
Anti-Mouse CD163 Percp eFluor710	eBioscience	Cat # 46-1631-80, RRID:AB_2716955
Anti-Mouse CD86 FITC	BD PharMingen	Cat # 553691, RRID:AB_394993
Anti-Mouse iNOS PE-Cy7	eBioscience	Cat # 25-5920-80, RRID:AB_2573498
Anti-Mouse F4/80 APC	Biolegend	Cat # 123116, RRID:AB_893481
Anti-Mouse B220 Alexa Fluor 700	BD PharMingen	Cat # 557957, RRID:AB_396957
Anti-Mouse CD3 Pacific Blue	BD PharMingen	Cat # 558214, RRID:AB_397063
Rat anti-mouse CD16/CD32	BD PharMingen	Cat # 553142, RRID:AB_394657
Anti-Mouse Ki67-FITC	eBioscience	Cat # 11-5698-82, RRID:AB_11151330
Ghost red 780 viability dye	Tonbo bioscience	Cat # 13-0865-T100
Chemicals, Peptides, and Recombinant Proteins		
Dextran Sulfate Sodium (DSS)	MP Biomedicals	Cat # 160110
Dulbecco's Modified Eagle's Medium (DMEM)	Corning	Cat # 10-013-CV
RPMI	Corning	Cat # 10-040-CV
Fetal bovine serum (FBS)	Sigma	Cat # F8067
Penicillin Streptomycin	Corning	Cat # 30-002-CI
L-glutamine	Corning	Cat # 25-005-CI
DPBS	Corning	Cat # 21-031-CV
Accutase	Corning	Cat # AT104
Trypsin	Corning	Cat # 25-052-CI
Murine IFNγ	R&D systems	Cat # 485-MI-100
Murine CXCL12	R&D systems	Cat # 460-SD
Murine CCL2	R&D systems	Cat # 479-JE-050
CCR2 antagonist (RS 102895)	Sigma	Cat # R1903
CXCR4 antagonist (AMD3100)	Sigma	Cat # A5602
Liposomal clodronate	Encapsula nanoscience	SKU # CLD-8909
Human Matrix metalloproteinase 1 (MMP1)	Sigma	Cat # SRP6269
Collagenase II	Worthington	Cat # LS00417
Dispase	Stem cell technologies	Cat # 07923
EDTA	Calbiochem	Cat # 324504
ECL substrate	Bio-Rad	Cat # 170-5060
Ethylene glycol bis(succinimidyl succinate (EGS)	Thermo Fisher Scientific	Cat # 21565

REAGENT or RESOURCE	SOURCE	IDENTIFIER
Pierce™ Protein A/G Magnetic Beads	Thermo Fisher Scientific	Cat # 88802
Amicon ultracentrifugal filter	Millipore	Cat # UFC700308
BD Cytofix/Cytoperm fixation and permeabilization buffer	BD Bioscience	Cat # 554722
Dynabeads Mouse T-Activator CD3/CD28	GIBCO, life technologies	Cat # 11452D
Critical Commercial Assays		
CCL2 ELISA Kit	Invitrogen	Cat # 554722
CXCL12 ELISA kit	R&D	Cat# MCX120
IL-10 ELISA	Invitrogen	Cat # 88-7105-88
Mouse chemokine array	R&D	Cat # ARY020
Mouse T cell isolation Kit	STEMCELL technologies	Cat # 19851
Experimental Models: Organisms/Strains		
B6.129P2-IL-10tm1cgn/J	Jackson Laboratory	Stock No. 002251
B6.129S4-Ccl2tm1Rol/J	Jackson Laboratory	Stock No. 004434
B6(Cg)-IL-10tm1.1Karp/J	Jackson Laboratory	Stock No. 014530
Software and Algorithms		
GraphPad Prism	GraphPad software, Inc	https://www.graphpad.com
FCS express version 6	FCS express	https://www.denovosoftware.com
Adobe illustrator cc 2017	Adobe	v21.0.2.242x64